

## Photonic bands and group-velocity dispersion in Si/SiO<sub>2</sub> photonic crystals from white-light interferometry

M. Galli, D. Bajoni, F. Marabelli, and L. C. Andreani

*Istituto Nazionale per la Fisica della Materia and Dipartimento di Fisica "A. Volta," Università di Pavia, Via Bassi 6, I-27100 Pavia, Italy*

L. Pavesi

*Istituto Nazionale per la Fisica della Materia and Dipartimento di Fisica, Università di Trento, Via Sommarive 18, I-38050 Povo, Italy*

G. Pucker

*Istituto di Ricerca Scientifica e Tecnologica, IRST-ITC, Via Sommarive 18, I-38050 Povo, Italy*

(Received 29 July 2003; revised manuscript received 19 December 2003; published 12 March 2004)

The phase delay of a light beam transmitted through (Si/SiO<sub>2</sub>)<sub>m</sub> multilayers with  $m = 2, 4, 6, 8$  is measured by white-light interferometry based on a fixed Mach-Zehnder interferometer coupled to a scanning Michelson interferometer. Results for photonic band and group velocity dispersion are obtained in a wide frequency spectrum and compare successfully with the predictions of electromagnetic theory. In particular, a strong slowing down of the group velocity at the band edges and superluminal propagation within the gap are demonstrated.

DOI: 10.1103/PhysRevB.69.115107

PACS number(s): 42.70.Qs, 42.30.Rx, 78.67.Pt, 95.75.Kk

### I. INTRODUCTION

Photonic crystals—namely, materials with a periodic dielectric constant—were introduced in 1987 by Yablonovitch<sup>1</sup> and John.<sup>2</sup> Soon afterwards, the first samples were fabricated in the microwave spectral range and the photonic band dispersion was measured by phase-sensitive techniques that yielded the wave vector in the sample at each given frequency.<sup>3,4</sup> These experimental determinations were of great importance for comparison with calculations of photonic bands by means of the vectorial plane-wave method.<sup>5,6</sup>

A current challenge is to fabricate and investigate photonic crystals in the near-infrared and visible regions. Several techniques for measuring the photonic band dispersion have been devised. In-plane transmission in two-dimensional (2D) waveguide-embedded photonic crystals has been used to map the photonic bands from Fabry-Perot fringes within the sample.<sup>7</sup> Another technique for measuring 2D photonic bands in a waveguide<sup>8,9</sup> relies on the observation of sharp structures in reflectance from the surface, which arise from coupling of the incoming radiation field to photonic modes. The same variable-angle reflectance technique can be applied even if no waveguide is present,<sup>10</sup> and in this case the photonic dispersion parallel to the crystal surface is measured. The band dispersion can also be determined from the refraction of a light beam.<sup>11</sup> Although these techniques are very useful, the phase-sensitive method<sup>3,4</sup> remains the most direct and conceptually simplest way to determine the photonic band dispersion in the direction of light propagation.

In this work we report on a measurement by means of white-light interferometry of photonic bands and group velocity in 1D Si/SiO<sub>2</sub> photonic crystals—i.e., distributed Bragg reflectors (DBR's). The experimental technique relies on a fixed white-light Mach-Zehnder interferometer coupled to a scanning Michelson interferometer and allows measuring the phase delay of a light beam through the sample in a

wide frequency spectrum: this represents the optical analog of the phase-sensitive determination of photonic bands demonstrated in Refs. 3 and 4. The derivative of the phase with respect to the frequency leads to the group velocity, which is found to have strong frequency dispersion, and to reach superluminal values within the photonic gap. The method is suitable to be applied to photonic crystals of higher dimensionalities.

Previous white-light determinations of the phase delay using a single interferometer have been reported<sup>12–14</sup>; in particular, the photonic dispersion has been determined for Fibonacci structures.<sup>15</sup> The photonic band dispersion of 3D photonic crystals close to the band edge has been studied in Refs. 16 and 17 by means of interferometry in the frequency domain. The present apparatus with two interferometers and time-domain Fourier analysis is closest to that of Refs. 18 and 19; however, in these papers a subpicosecond laser pulse is used as a source. As a result, using an ultrashort pulse can lead to the phase dispersion in a relatively narrow frequency window<sup>18</sup> but finds a most natural and powerful application for time-resolved experiments: indeed, time-resolved interferometric studies of colloidal photonic crystals<sup>19</sup> and of 1D Fibonacci multilayers<sup>20</sup> yielded useful information on pulse distortion and slowing down of wave packets close to the band edge. On the other hand, the present approach based on cw white light is most suited for a frequency-resolved determination of phase delay and group velocity in a wide spectral range.

The paper is organized as follows. In Sec. II a short description of the samples and of transmittance spectra is presented. Section III gives an account of the white-light interferometric technique. In Sec. IV we present the physical results for photonic bands and group velocity, together with a comparison with a theoretical treatment. In Sec. V we summarize the main results.

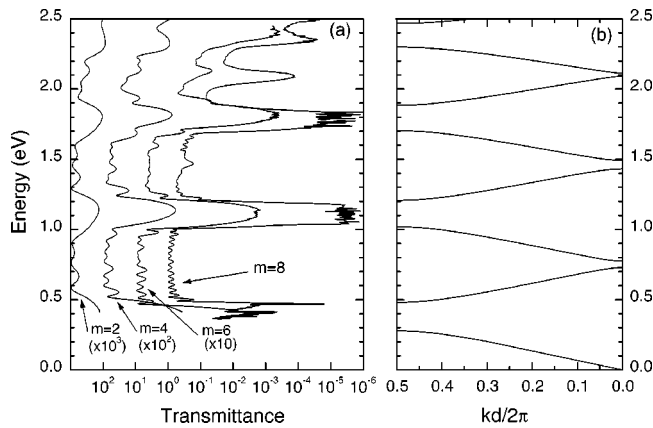


FIG. 1. (a) Transmittance spectra for samples with a different number  $m$  of periods and (b) calculated photonic bands for the infinite multilayer. Transmittance spectra are horizontally shifted by the values reported in parentheses for clarity.

## II. SAMPLES AND TRANSMITTANCE SPECTRA

Si/SiO<sub>2</sub> multilayers were grown in a low-pressure chemical vapor deposition system on a 4-in. SiO<sub>2</sub> wafer. Reproducible and uniform layers were obtained by a processing approach based on a three-step procedure.<sup>21,22</sup> First, poly-Si was deposited on a SiO<sub>2</sub> wafer at 620 °C and with SiH<sub>4</sub> pressure of 280 mTorr. Then, the poly-Si layer was thinned to about 230 nm by wet oxidation (in H<sub>2</sub>, O<sub>2</sub>) at 975 °C. This etching procedure resulted in an additional growth of 140 nm of *a*-SiO<sub>2</sub> on the poly-Si layer. Further enlargement of the SiO<sub>2</sub> layer was then obtained by deposition of 500 ± 15 nm SiO<sub>2</sub> (using tetra-ethyl-orthosilicate, at 718 °C). These three steps were repeated to obtain (Si/SiO<sub>2</sub>)<sub>*m*</sub> multilayers with number of periods  $m=2, 3, 4, 6, 8$  and with nominal layer thicknesses of 229 nm and 658 nm for poly-Si and SiO<sub>2</sub> layers, respectively. These values correspond to  $\lambda/4$  DBR's—i.e., with the thickness of each layer being inversely proportional to its refractive index.

The experimental transmittance ( $T$ ) spectra of (Si/SiO<sub>2</sub>)<sub>*m*</sub> multilayers with  $m=2, 4, 6, 8$  are shown in Fig. 1(a) on a semilogarithmic scale. All the samples exhibit similar features which are typical of the optical response of a 1D photonic structure. In particular, two major minima in  $T$  which correspond to the principal stop bands are observed at 1.14 and 1.81 eV, respectively. These can be classified as odd-order gaps—i.e., stop bands that lie at the Brillouin zone edge. Additionally, weaker transmission minima corresponding to gaps of even order—i.e., stop bands at the center of the Brillouin zone—are also observed at 0.67 and 1.39 eV. As predicted from the theory for  $\lambda/4$  multilayers, forbidden gaps of odd order are wider than even-order ones. Thus even-order gaps have lower attenuation and are more sensitive to the structural disorder present in the samples, resulting in less evident structures in  $T$  spectra. The amplitude and shape of the stop bands are drastically modified by increasing the number of periods  $m$ . For large  $m$  values they become deeper and assume a steplike shape at the gap edges, indicating an improved rejection ratio. Finally, for energies greater than 1.5 eV, the absorption from poly-Si becomes

relevant and increases with  $m$  due to increasing total poly-Si thickness; beyond 3 eV, the transmittance intensity reduces practically to zero for all samples.

The calculated 1D photonic band dispersion is shown in Fig. 1(b). This is obtained from the well-known secular equation for a 1D periodic structure<sup>23</sup>:

$$\cos kd = \cos k_1 L_1 \cos k_2 L_2 - \frac{1}{2} \left( \frac{n_1}{n_2} + \frac{n_2}{n_1} \right) \sin k_1 L_1 \sin k_2 L_2, \quad (1)$$

where  $k$  is the Bloch vector along the multilayer axis,  $d = L_1 + L_2$  is the period, and  $L_j$ ,  $n_j$ , and  $k_j = n_j \omega / c$  ( $j = 1, 2$ ) are the thickness, refractive index, and wave vector in the layer  $j$ , respectively.<sup>24</sup> The frequency dependence of  $n$  is taken into account (except for the optical phonon resonance of SiO<sub>2</sub> around 0.15 eV). The calculated photonic gap positions match very well the  $T$  minima. It can be seen that photonic gaps of even order are very narrow: indeed they should disappear for a  $\lambda/4$  DBR in the case of no material dispersion.

## III. WHITE-LIGHT INTERFEROMETRY

The phase shift of the light transmitted through the multilayer samples is obtained experimentally by means of white-light interferometry in the time domain. This technique has been successfully applied in the past years to study the dispersion characteristics of transparent media with high temporal and spectral resolution;<sup>12–14</sup> however, the use of a single interferometer in these works resulted in the determination of the group delay (i.e., the derivative of the phase with respect to frequency) from a fit to the measured phase data. Similar remarks can be made for the frequency-domain interferometric studies of Refs. 16 and 17, which focus on the photonic dispersion close to the band edge. In the present work, the use of a double-interferometer configuration leads to a direct and precise determination of the phase dispersion and also of the group velocity.

The experimental setup, which has been thoroughly discussed in Ref. 25, consists in a modified Mach-Zehnder interferometer (MZI) coupled to a commercial scanning Michelson interferometer (SMI, model Bruker IFS 66/S). White light from a tungsten-halogen lamp is sent to the MZI in order to produce two identical light beams (hereafter referred to as the “sample” and “reference” beams) with a given optical path difference  $\Delta L$ . If a sample of thickness  $D$  is inserted in one arm of the MZI, the phase difference between the two arms can be written as

$$\Delta \phi(\omega) = \phi(\omega) - \frac{\omega}{c} D + \frac{\omega}{c} \Delta L \equiv \theta(\omega) + \frac{\omega}{c} \Delta L, \quad (2)$$

where  $\phi(\omega)$  is the phase delay introduced by the sample: it can be expressed as  $\phi(\omega) = k(\omega)D$ , where  $k(\omega)$  is the wave vector in the sample at the given frequency. As discussed by Kop and Sprik<sup>18</sup> and shown below,  $\Delta \phi(\omega)$  can be precisely determined by applying Fourier-transform analysis of the interferogram observed at the output of the MZI. Once the sample parameter  $D$  is known and  $\Delta L$  is determined via a

reference measurement without the sample, the phase shift  $\phi(\omega)$  can be directly determined. At variance with Ref. 18, where an ultrashort laser pulse was used as a source, the analysis and method can be successfully applied also when a broadband, incoherent white-light source is used.

If we describe the Fourier components of the electric field in the reference beam by  $A(\omega)$  and we let  $H(\omega) = H_0(\omega)e^{i\theta(\omega)}$  be the transfer function which describes the sample response, then the total electric field  $E(t)$  at the output of the MZI may be expressed as

$$E(t) = \int_{-\infty}^{+\infty} [A(\omega)e^{i\omega t} + H(\omega)A(\omega)e^{i\omega(t+\Delta L/c)}] d\omega, \quad (3)$$

where  $\Delta L/c$  is the time delay between the two arms of the MZI. The complex amplitude functions  $A(\omega)$  and  $H(\omega)$  describe both the power spectrum and the relative phase relation between the frequency components of the reference and sample beams. The overall intensity and phase information on a given sample can be directly accessed by scanning the time delay between the two beams by means of a standard Fourier-transform interferometer.

Analytically, the interferogram  $I(\tau)$  should be obtained by the integral of the electric field  $E(t-\tau)$  over the whole spectral domain of the light source:

$$\begin{aligned} I(\tau) &= \int_{-\infty}^{+\infty} E(t)E^*(t-\tau) dt \\ &= \int_{-\infty}^{+\infty} H(\omega)^* |A(\omega)|^2 e^{i\omega(\tau-\Delta L/c)} d\omega \\ &\quad + \int_{-\infty}^{+\infty} (|A(\omega)|^2 + |H(\omega)A(\omega)|^2) e^{i\omega\tau} d\omega \\ &\quad + \int_{-\infty}^{+\infty} H(\omega) |A(\omega)|^2 e^{i\omega(\tau+\Delta L/c)} d\omega. \end{aligned} \quad (4)$$

The second integral on the right-hand side describes the autocorrelation signal, while the first and third integrals describe the cross-correlation parts of the interferogram. By taking the Fourier transform of one of the cross-correlation terms and using Eq. (2) one obtains

$$\bar{I}(\omega) = H_0(\omega) |A(\omega)|^2 e^{i\Delta\phi(\omega)}. \quad (5)$$

This equation simply yields the spectral dependence of the phase difference as  $\Delta\phi(\omega) = \text{Im} \ln \bar{I}(\omega)$ . The quantity  $\theta(\omega) = \phi(\omega) - (\omega/c)D$  is determined experimentally by subtracting the phase difference measured with the sample [ $\Delta\phi(\omega)$ ] and without the sample [ $\omega\Delta L/c$ ]; the phase delay  $\phi(\omega)$  is then trivially obtained by adding  $\omega D/c$ . The uninteresting phase introduced by the SiO<sub>2</sub> substrate common to all samples is measured separately on a substrate and the result is subtracted from the phase measured on the samples.

A typical interferogram observed after passing through the SMI is shown in Fig. 2. It is characterized by a central structure and two specular and identical satellite structures (the one for negative delays is not shown in Fig. 2). The first one is given by the autocorrelation signal, while the second ones result from the cross correlation between the sample

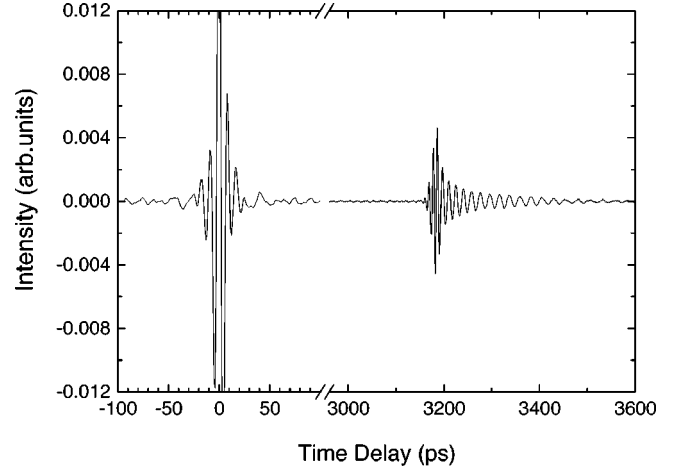


FIG. 2. Typical interferogram for the eight-period sample (note the different time scales of the two components). The central autocorrelation part is nearly symmetric. Only the cross-correlation part at positive time delay is shown, the one at negative time delay being specular with respect to the zero.

and reference arms of the MZI. As evidenced in Fig. 2, while the autocorrelation peak is symmetric, the right- and left-hand-side cross-correlation peaks show a pronounced elongation towards positive and negative time delays, respectively. This reflects the dispersion characteristics of the sample—i.e., the wavelength-dependent phase delay. The time separation  $\Delta t = \Delta L/c$  between the satellite peaks and the central one is just the time delay between the two arms of the MZI. This time delay can be adjusted by changing  $\Delta L$  through a suitable delay line in the MZI. This adjustment is convenient in order to separate the satellite from the central interferograms and to achieve a better resolution for the Fourier transform leading to the phase determination.

We note two important advantages of this experimental procedure: (i) The absolute phase shift introduced by the sample is obtained by subtracting the results of two successive measurements. This way any spurious instrumental contribution is canceled out. (ii) The cross-correlation part of the interferogram is always measured simultaneously with the autocorrelation one. Therefore the time delay introduced by the sample is automatically referenced to the zero-delay point (i.e., by the central autocorrelation part of the interferogram) with a high degree of accuracy. These two features, together with the high stability and reproducibility of the commercial SMI, lead to a remarkable accuracy in the determination of the spectral dependence of the phase shift in addition to its derivatives. The typical time resolution is of the order of  $10^{-2}$  fs which translates into an accuracy of about  $10^{-2}$  rad (at  $\lambda = 1 \mu\text{m}$ ) in the phase determination.

#### IV. RESULTS FOR PHASE AND GROUP VELOCITY DISPERSION

In Fig. 3 we show the phase delay  $\phi(\omega)$  measured for the  $m=6$  and  $m=8$  multilayers in the region of the band gap centered around 1.14 eV. The phase delay is obviously larger for the thicker sample. The photonic gap can be recognized

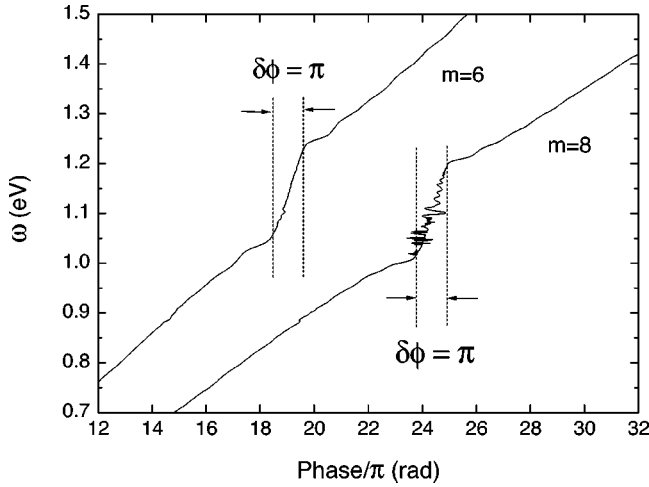


FIG. 3. Measured phase delay  $\phi(\omega)$  (in units of  $\pi$ ) through the  $m=6$  and  $m=8$  samples. The vertical dashed lines denote the phase change across the photonic gap.

as the energy window in which the phase dispersion has a pronounced change in slope, and it relates to the region of low transmission shown in Fig. 1. The behavior for the  $m=8$  sample in the gap is more noisy due to the very low transmission, but the trend is the same as that of the  $m=6$  sample. Note that the *change* in phase across the photonic gap is the same for both samples and it equals  $\pi$  within the experimental uncertainty. The theory of multilayers is usually developed for reflection<sup>23,26,27</sup> and it leads to a similar property—namely, that the phase of the reflection amplitude changes by  $\pi$  from the lower to the upper edge of a photonic gap. The present experimental results are consistent with numerical calculations of the phase in transmission to be discussed below.

In Fig. 4 we show the experimental results for the phase delay and group velocity for all investigated samples with number of periods  $m=2,4,6,8$ . The left panels display the phase  $\phi/(2\pi m)$ —i.e., after dividing by the number of periods: this quantity can be identified with  $kd/2\pi$ , where  $k$  is the wave vector of the 1D periodic system in the extended zone scheme. The measurements map the wave vector from the second to the fifth Brillouin zone: the boundaries of the Brillouin zones are shown by dotted lines on the result for the  $m=8$  sample, which is the closest to the ideal periodic system. Thus the results of the phase measurement represent a determination of the band dispersion for the 1D photonic crystal,<sup>28</sup> in analogy with previous determinations in the microwave spectral region.<sup>3,4</sup> The identification of the phase delay with the band dispersion for the infinite photonic crystal becomes increasingly more precise for samples with higher number of periods. Thanks to the large refractive index contrast between Si and SiO<sub>2</sub>, the sample with  $m=8$  is already seen to reproduce the band dispersion of the periodic system shown in Fig. 1(b). The most critical feature to reproduce is the flattening of the 1D photonic bands at the band edges: this feature becomes more pronounced in the group velocity curves to be discussed below.

The right panels in Fig. 4 display the inverse of the group velocity in units of the speed of light  $c$ , which is obtained as

$$\frac{c}{v_g} = \frac{c}{D} \frac{d\phi}{d\omega}. \quad (6)$$

The group velocity in the energy region of photonic bands has oscillations around the value  $c/\bar{n}$ , where  $\bar{n}$  is an effective refractive index. A maximum in the group velocity corresponds to the excitation of a Bloch-Floquet mode in the multilayer and also to a maximum of transmission. The oscillations due to the presence of Bloch modes in the finite multilayer give rise also to finer features in the phase dispersion (Fig. 3 and left panels in Fig. 4). The quantity  $c/v_g$  has strong peaks at the band edges, which become more pronounced on increasing the number of period. These peaks reflect the flattening of the photonic bands at the Brillouin zone edges and the consequent vanishing of the group velocity, as implied by the photonic bands of Fig. 1(b). Moreover, inside the photonic gap around 1.1 eV the group velocity displays superluminal values (for the samples with  $m=6$  and  $m=8$ ). As is well known, this electromagnetic phenomenon is not in contrast with the causality principle<sup>29–32</sup>: indeed the physically relevant quantity is the velocity  $v_E$  of energy transport, which coincides with  $v_g$  only when the transmission coefficient is unity.<sup>33</sup> In fact superluminal behavior is restricted to an energy window of strong extinction. Nevertheless, we stress that the experimental results of Fig. 4 represent a direct determination both of slowing down of a wave packet at the band edge and of superluminal propagation in the gap for monochromatic waves: both phenomena are of considerable interest for nonlinear and pulse propagation effects.<sup>34,35</sup>

Figure 5 shows the results of theoretical calculations of the same quantities shown in Fig. 4—namely, the phase  $\phi/2\pi m \equiv kd/2\pi$  (left) and the inverse of the group velocity  $c/v_g$  (right). The results for  $m=\infty$ —i.e., for the infinite system—are also shown. All curves take into account the material dispersion of the dielectric functions. As can be noticed by a comparison between Figs. 4 and 5, the calculated curves correspond quite well to the experimental data. The small differences in the detailed behavior of the group velocity oscillations may be traced to lateral inhomogeneities in the sample, which are partially taken into account by introducing a Gaussian broadening. The formation of the band dispersion and of the photonic gaps, slowing down of  $v_g$  at the band edge, and superluminal propagation in the gaps are all reproduced. In particular, it is interesting to notice the fine features in the phase dispersion for the finite structures, which correspond closely to the  $c/v_g$  oscillations. In fact the phase change across a photonic mode equals  $\pi$  in both experiment and calculations, as expected from general scattering theory.

It is interesting to discuss the electromagnetic properties of the finite multilayer structure and the evolution towards the limit of an infinite photonic crystal. The photonic bands of the periodic 1D system are discretized in a multilayer with  $m$  periods due to the boundary conditions on the photonic Bloch modes. Between two successive band gaps [i.e., in a range  $(n-1)\pi < kd < n\pi$  with integer values of  $n$ ] there are exactly  $m-1$  values of the Bloch vector  $k$ , which are given by  $kd = (n-1)\pi + j\pi/m$ ,  $j=1, \dots, m-1$ . The correspond-

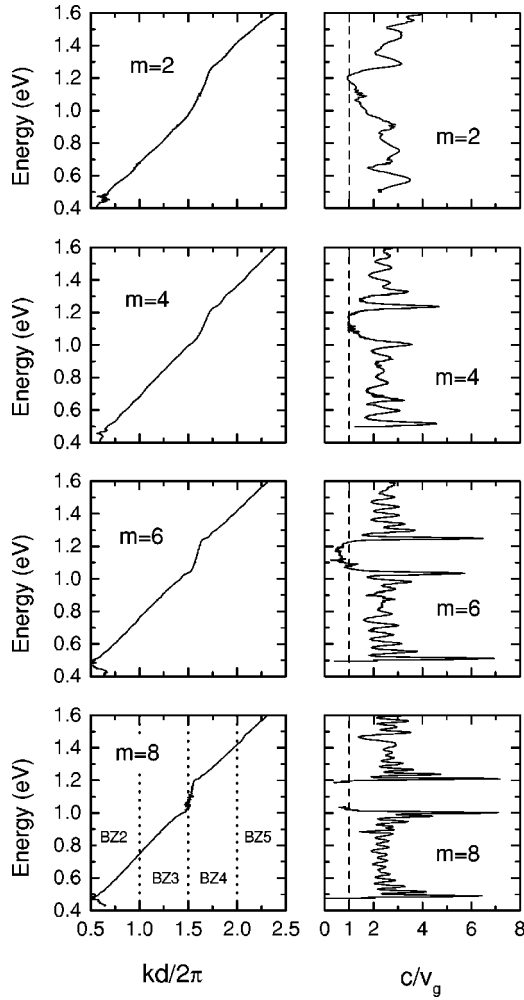


FIG. 4. Experimental results for the phase delay  $\phi/2\pi m \equiv kd/2\pi$  (left) and inverse of the group velocity (right) for samples with different numbers of periods. Boundaries of the Brillouin zones (BZ2—BZ5) are indicated by dotted lines for the sample with  $m=8$ .

ing Bloch-Floquet modes are clearly visible as sharp maxima in the transmission spectra of Fig. 1(a) and in the  $c/v_g$  curves of Figs. 4 and 5 (right panels). The envelope of the closely spaced oscillations in the inverse group velocity goes over to the curve for the infinite system shown in Fig. 5 (right bottom panel). Finite-size oscillations are also present but less evident in the phase dispersion curves of Figs. 4 and 5 (left panels), which evolve smoothly towards the photonic band dispersion for the periodic system shown in Fig. 5 (left bottom panel).

A very important quantity is the maximum slowing down of the group velocity that can be attained close to the band edge (which also leads to strongly enhanced nonlinear effects<sup>33–35</sup>). The Bloch-Floquet mode lying closest to a band edge, also called the *band-edge resonance*, has the smallest value of  $v_g/c$  among the  $m-1$  discretized modes. The behavior of the group velocity as a function of the number of periods has been studied by means of detailed scattering-theory calculations.<sup>36</sup> The quantity  $c/v_g$  (which is called the

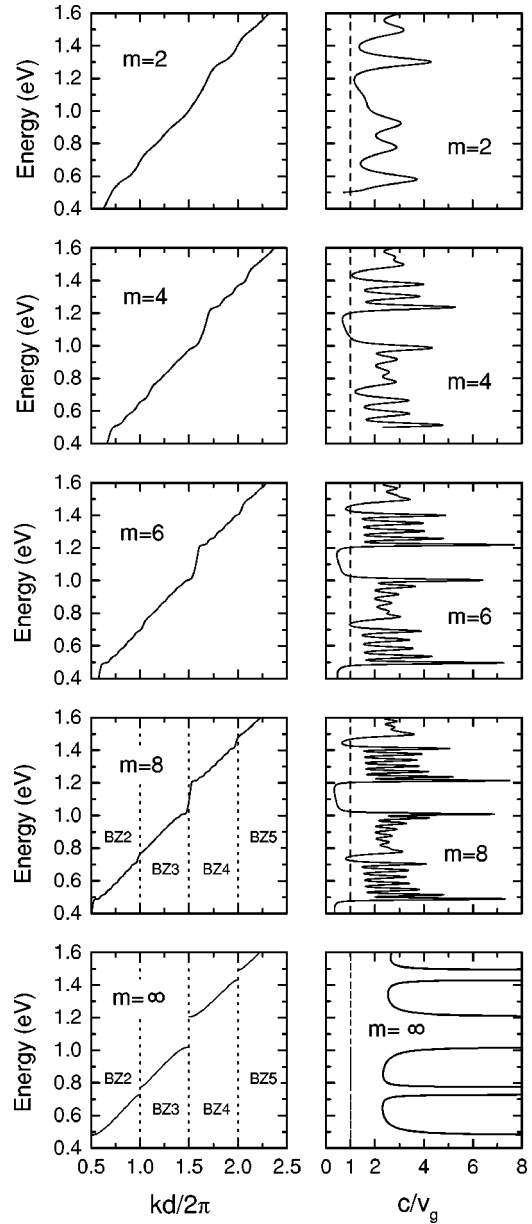


FIG. 5. Theoretical results for the phase  $\phi/2\pi m \equiv kd/2\pi$  (left) and inverse of the group velocity (right) for samples with different numbers of periods and for the ideal infinite photonic crystal ( $m = \infty$ ). The curves in the right panels for  $m=2,4,6,8$  have been convoluted with a Gaussian line shape with a full width at half maximum of 4 meV.

density of optical modes in Ref. 36) is always finite in a system of finite size and for the band-edge resonance it grows proportionally to  $m^2$  for large  $m$ . In a real sample, the maximum slowing down at the band edge is limited not only by the finite number of periods, but also by inhomogeneous broadening caused by sample imperfections. In the present experiments the broadening parameter is found to be of the order of 4 meV, which is taken into account in the calculated  $c/v_g$  curves of Fig. 5 by means of a Gaussian line shape convolution (this is the reason why the maximum  $c/v_g$  does not increase in going from  $m=6$  to  $m=8$  periods). The ef-

fect of inhomogeneous broadening limits the slowing down to  $c/v_g \sim 7$  in the present experiments, as it appears from Fig. 4.

Concerning the superluminal velocity in the band gap, the results of Ref. 36 indicate that  $c/v_g$  at midgap is proportional to  $m^{-1}$  for large  $m$ . This behavior can be simply understood as follows. The variation of the phase delay across the photonic gap equals  $\pi$  for any number of periods, as is shown in Fig. 3 and reproduced by the theoretical results of Fig. 5. Assuming the phase dispersion to be linear within the gap and using Eq. (6) with  $D = md$  leads to the approximate formula

$$\frac{v_g}{c} = m \frac{d\Delta\omega_g}{\pi c}, \quad (7)$$

where  $\Delta\omega_g$  is the gap width.<sup>37</sup> For the present case with  $d = 835$  nm and  $\Delta\omega_g \approx 0.2$  eV for the third-order gap we get  $v_g/c \approx 0.27m$ , leading to a superluminal group velocity for  $m \geq 4$ , in agreement with the theoretical curves of Fig. 5. Experimentally, the group velocity is found to become superluminal for the samples with  $m = 6$  and  $m = 8$ , the lack of superluminal behavior for  $m = 4$  being probably due to inhomogeneous broadening effects within the gap which go beyond the simple Gaussian line shape model.

## V. CONCLUSIONS

The white-light interferometric technique has been successfully applied to a measurement of the phase delay and

group velocity dispersion of 1D photonic crystals in a wide spectral range. The use of a fixed Mach-Zehnder interferometry in combination with a scanning Michelson interferometer results in a very precise determination of the phase delay through the sample. The high experimental accuracy allows us to resolve the fine details of the phase behavior and of the photonic band formation in the finite multilayers investigated.

Results for Si/SiO<sub>2</sub> photonic crystals validate the behavior expected from electromagnetic theory; in particular, it is shown experimentally that the change in transmission phase across the photonic gap equals  $\pi$  for samples with a different number of periods. The results for the phase dispersion show the formation of photonic bands in the extended-zone scheme with fine features associated with the presence of photonic Bloch modes confined in the finite structure. The group velocity displays wide variations as predicted by theory, including peculiar features like strong slowing down at the band edge and superluminal behavior within the photonic gap. These phenomena are observed in the near-infrared and visible spectral regions. The same method can be applied in principle to two- and three-dimensional photonic crystals, as well as to filter and microcavity structures.

## ACKNOWLEDGMENTS

Useful discussions with M. Belotti, G. Guizzetti, G. La Rocca, and M. Patrini are gratefully acknowledged. This work was supported by MIUR through Cofin program.

- 
- <sup>1</sup>E. Yablonovitch, Phys. Rev. Lett. **58**, 2059 (1987).  
<sup>2</sup>S. John, Phys. Rev. Lett. **58**, 2486 (1987).  
<sup>3</sup>E. Yablonovitch and T.J. Gmitter, Phys. Rev. Lett. **63**, 1950 (1989).  
<sup>4</sup>W.M. Robertson, G. Arjavalingam, R.D. Meade, K.D. Brommer, A.M. Rappe, and J.D. Joannopoulos, Phys. Rev. Lett. **68**, 2023 (1992); J. Opt. Soc. Am. B **10**, 322 (1993).  
<sup>5</sup>K.M. Leung and Y.F. Liu, Phys. Rev. Lett. **65**, 2646 (1990); Z. Zhang and S. Satpathy, *ibid.* **65**, 2650 (1990); K.M. Ho, C.T. Chan, and C.M. Soukoulis, *ibid.* **65**, 3152 (1990); P.R. Villeneuve and M. Piché, Phys. Rev. B **46**, 4969 (1992); R.D. Meade, K.D. Brommer, A.M. Rappe, and J.D. Joannopoulos, Appl. Phys. Lett. **61**, 495 (1992).  
<sup>6</sup>J.D. Joannopoulos, R.D. Meade, and J.N. Winn, *Photonic Crystals* (Princeton University Press, Princeton, 1995).  
<sup>7</sup>D. Labilloy, H. Benisty, C. Weisbuch, C.J.M. Smith, T.F. Krauss, R. Houdré, and U. Oesterle, Phys. Rev. B **59**, 1649 (1999).  
<sup>8</sup>T. Fujita, Y. Sato, T. Kuitani, and T. Ishihara, Phys. Rev. B **57**, 12 428 (1998).  
<sup>9</sup>V.N. Astratov, D.M. Whittaker, I.S. Culshaw, R.M. Stevenson, M.S. Skolnick, T.F. Krauss, and R.M. De La Rue, Phys. Rev. B **60**, R16 255 (1999).  
<sup>10</sup>M. Galli, M. Agio, L.C. Andreani, M. Belotti, G. Guizzetti, F. Marabelli, M. Patrini, P. Bettotti, L. Dal Negro, Z. Gaburro, L. Pavesi, A. Lui, and P. Bellutti, Phys. Rev. B **65**, 113111 (2002).  
<sup>11</sup>M. Notomi, T. Tamamura, Y. Ohtera, O. Hanaizumi, and S. Kawakami, Phys. Rev. B **61**, 7165 (2000).  
<sup>12</sup>M. Beck and I.A. Walmsley, Opt. Lett. **15**, 492 (1990).  
<sup>13</sup>K. Naganuma, K. Mogi, and H. Yamada, Opt. Lett. **15**, 393 (1990).  
<sup>14</sup>S. Diddams and J.C. Diels, J. Opt. Soc. Am. B **13**, 1120 (1996).  
<sup>15</sup>T. Hattori, N. Tsurumachi, S. Kawato, and H. Nakatsuka, Phys. Rev. B **50**, R4220 (1994).  
<sup>16</sup>I.I. Tarhan, M.P. Zinkin, and G.H. Watson, Opt. Lett. **20**, 1571 (1995).  
<sup>17</sup>B.T. Rosner, G.J. Schneider, and G.H. Watson, J. Opt. Soc. Am. B **15**, 2654 (1998).  
<sup>18</sup>R.H.J. Kop and R. Sprik, Rev. Sci. Instrum. **66**, 5459 (1995).  
<sup>19</sup>A. Imhof, W.L. Vos, R. Sprik, and A. Lagendijk, Phys. Rev. Lett. **83**, 2942 (1999).  
<sup>20</sup>L. Dal Negro, C.J. Oton, Z. Gaburro, L. Pavesi, P. Johnson, A. Lagendijk, R. Righini, M. Colocci, and D.S. Wiersma, Phys. Rev. Lett. **90**, 055501 (2003).  
<sup>21</sup>G. Pucker, P. Bellutti, C. Spinella, K. Gatterer, M. Cazzanelli, and L. Pavesi, J. Appl. Phys. **88**, 6044 (2000).  
<sup>22</sup>M. Patrini, M. Galli, M. Belotti, L.C. Andreani, G. Guizzetti, G. Pucker, A. Lui, P. Bellutti, and L. Pavesi, J. Appl. Phys. **92**, 1816 (2002).  
<sup>23</sup>A. Yariv and P. Yeh, *Optical Waves in Crystals* (Wiley, New York, 1984).

- <sup>24</sup>The layer thicknesses used in the calculation were 220 nm for Si and 615 nm for SiO<sub>2</sub>, as determined from a best fit to the ellipsometric data (Ref. 22).
- <sup>25</sup>M. Galli, F. Marabelli, and G. Guizzetti, *Appl. Opt.* **42**, 3910 (2003).
- <sup>26</sup>H.A. McLeod, *Thin-Film Optical Filters*, 2nd ed. (Hilger, London, 1986).
- <sup>27</sup>D.I. Babic and S.W. Corzine, *IEEE J. Quantum Electron.* **28**, 514 (1992).
- <sup>28</sup>We recall that the photonic band dispersion discussed here refers only to a wave vector along the multilayer axis, while the bands retain a smooth and positive dispersion for a wave vector component in the  $xy$  plane. This prevents the system from behaving as a negative refractive material. Only for light incident from the sample side (i.e., in the geometry of diffraction by a 1D grating) would it be possible to have a diffracted light beam in the backwards direction. However, as discussed by M. Notomi [*Phys. Rev. B* **62**, 10 696 (2000)] this cannot be properly called negative refraction and can in no way be characterized by a negative refractive index, both phenomena being possible only for 2D or 3D photonic crystals.
- <sup>29</sup>A.M. Steinberg, P.G. Kwiat, and R.Y. Chiao, *Phys. Rev. Lett.* **71**, 708 (1993).
- <sup>30</sup>Ch. Spielmann, R. Szipöcs, A. Stingl, and F. Krausz, *Phys. Rev. Lett.* **73**, 2308 (1994).
- <sup>31</sup>V. Romero-Rochín, R.P. Duarte-Zamorano, S. Nilsen-Hofseth, and R.G. Barrera, *Phys. Rev. E* **63**, 027601 (2001).
- <sup>32</sup>N.-H. Liu, S.-Y. Zhu, H. Chen, and X. Wu, *Phys. Rev. E* **65**, 046607 (2002).
- <sup>33</sup>G. D'Aguanno, M. Centini, M. Scalora, C. Sibilia, M.J. Bloemer, C.M. Bowden, J.W. Haus, and M. Bertolotti, *Phys. Rev. E* **63**, 036610 (2001); M. Centini, M. Bloemer, K. Myneni, M. Scalora, C. Sibilia, M. Bertolotti, and G. D'Aguanno, *ibid.* **68**, 016602 (2003).
- <sup>34</sup>M. Centini, C. Sibilia, M. Scalora, G. D'Aguanno, M. Bertolotti, M.J. Bloemer, C.M. Bowden, and I. Nefedov, *Phys. Rev. E* **60**, 4891 (1999).
- <sup>35</sup>Y. Dumeige, I. Sagnes, P. Monnier, P. Vidakovic, I. Abram, C. Mériadec, and A. Levenson, *Phys. Rev. Lett.* **89**, 043901 (2002).
- <sup>36</sup>J.M. Bendickson, J.P. Dowling, and M. Scalora, *Phys. Rev. E* **53**, 4107 (1996).
- <sup>37</sup>For a  $\lambda/4$  multilayer, expanding Eq. (1) close to a Brillouin zone edge leads to the approximate but rather accurate formula  $\Delta\omega_g = 2c|n_1 - n_2|/[n_1 L_1(n_1 + n_2)]$  for the width of odd-order gaps (Ref. 23).